

Accepted Manuscript

Ozone-Cathode Microbial Desalination Cell; an Innovative Option to Bioelectricity Generation and Water Desalination

Abdolmajid Gholizadeh, Ali Asghar Ebrahimi, Mohammad Hossein Salmani, Mohammad Hassan Ehrampoush



PII: S0045-6535(17)31422-4

DOI: 10.1016/j.chemosphere.2017.09.009

Reference: CHEM 19879

To appear in: *Chemosphere*

Received Date: 22 July 2017

Revised Date: 01 September 2017

Accepted Date: 02 September 2017

Please cite this article as: Abdolmajid Gholizadeh, Ali Asghar Ebrahimi, Mohammad Hossein Salmani, Mohammad Hassan Ehrampoush, Ozone-Cathode Microbial Desalination Cell; an Innovative Option to Bioelectricity Generation and Water Desalination, *Chemosphere* (2017), doi: 10.1016/j.chemosphere.2017.09.009

This is a PDF file of an unedited manuscript that has been accepted for publication. As a service to our customers we are providing this early version of the manuscript. The manuscript will undergo copyediting, typesetting, and review of the resulting proof before it is published in its final form. Please note that during the production process errors may be discovered which could affect the content, and all legal disclaimers that apply to the journal pertain.

Highlights:

- A new type of electron acceptors, ozone, was evaluated in MDCs.
- 16S rRNA gene sequencing and SEM images used to observe microbial community.
- Salinity removal efficiency above 74% was observed in the O₃-MDC.
- O₃-MDC produced power density of 11 times higher than O₂-MDC.
- *Proteobacteria* are from the dominant microbial communities in anode biofilm.

1 **Ozone-Cathode Microbial Desalination Cell; an Innovative Option**
2 **to Bioelectricity Generation and Water Desalination**

3 Abdolmajid Gholizadeh^{a,b}, Ali Asghar Ebrahimi^a, Mohammad Hossein Salmani^a, Mohammad
4 Hassan Ehrampoush^{*a}

5 ^a Ph.D., Environmental Science and Technology Research Center, Department of Environmental
6 Health Engineering, Shahid Sadoughi University of Medical Sciences, Yazd, Iran.

7 ^b Esfarayen faculty of medical sciences, Esfarayen, Iran

8 **Corresponding author:**

9 Mohammad Hassan Ehrampoush, Professor

10 Department of Environmental Health Engineering, Shahid Sadoughi University of Medical
11 Sciences, Yazd, Iran

12 Tel: +98-353-8209100

13 Email: ehram1334@gmail.com, ehrampoush@ssu.ac.ir

14 **Running title:** Ozone-Cathode Microbial Desalination Cell

15 **Ozone-Cathode Microbial Desalination Cell; an Innovative Option**
16 **to Bioelectricity Generation and Water Desalination**

17 Abdolmajid Gholizadeh^{a,b}, Ali Asghar Ebrahimi^a, Mohammad Hossein Salmani^a, Mohammad Hassan
18 Ehrampoush^{*a}

19 ^a Ph.D., Environmental Science and Technology Research Center, Department of Environmental Health
20 Engineering, Shahid Sadoughi University of Medical Sciences, Yazd, Iran.

21 ^b Esfarayen faculty of medical sciences, Esfarayen, Iran

22 *Corresponding author: Professor, Email: ehram1334@gmail.com

23 **Abstract**

24 Microbial desalination cell (MDC) is a new approach of water desalination methods, which is based on
25 ionic species removal from water in proportion to the electric current generated by bacteria. However, the
26 low current generation and insufficient deionization in this technology have created challenges to improve
27 the process. Here, the performance of MDC using ozone as a new electron acceptor (O₃-MDC) was
28 evaluated versus another operated independently with oxygen (O₂-MDC). Results showed the maximum
29 open-circuit voltages of 628 and 1331 mV for 20 g L⁻¹ NaCl desalination in O₂-MDC and O₃-MDC,
30 respectively. The O₃-MDC produced a maximum power density of 4.06 W m⁻² (about 11 times higher
31 than O₂-MDC) while at the same time was able to remove about 74% of salt (55.58% in the O₂-MDC).
32 Each cycle of O₂-MDC and O₃-MDC operation lasted about 66 and 94 h, respectively, indicating a more
33 stable current profile in the O₃-MDC. Moreover, sequencing test based on 16S rRNA gene showed that
34 the anode biofilm had more diverse microbial community than anolyte sample. Proteobacteria, Firmicutes
35 and Acidobacteria were from dominant microbial communities in anode biofilm sample. Accordingly, the
36 results revealed that ozone can enhance MDC performance either as a desalination process or as a pre-
37 treatment reactor for downstream desalination processes.

38 Key words: Ozonation; Microbial desalination cell (MDC); Electricity generation

39 1. Introduction

40 Safe drinking water is an essential for humans and other living beings. As the population grows, the
41 scarcity of fresh water resources and the demand for additional water supplies will be critical in many arid
42 regions around the world (Kim and Logan, 2013; Sevda et al., 2015). To overcome these problems, the
43 need for water desalination has increased recently, especially in the areas where the freshwater resources
44 are limited and brine/sea water is available (Sevda et al., 2015; Gholizadeh et al., 2017).

45 There are a number of commercial techniques for water desalination such as reverse osmosis (RO),
46 Nanofiltration (NF), electrodialysis (ED), ion-exchange resins, and etc., (Burn et al., 2015). However, one
47 of the drawbacks attributed to the current desalination technologies is their high-energy consumption,
48 resulted in high operating and water cost. For example, RO in a large scale is considered as one of the
49 most conventional desalination technologies which requires 3–7 kWh of energy to produce 1 m³ of fresh
50 water (Ping et al., 2014; Burn et al., 2015).

51 Recently, the bio-electrochemical systems (BESs) have emerged as the new technology for water and
52 wastewater treatment because of their relatively lower cost and environmental impacts (Logan et al.,
53 2006; Sevda et al., 2015; Sevda et al., 2017). A new BES for partial or complete water desalination is the
54 microbial desalination cell (MDC), which integrates microbial fuel cell (MFC) and electrodialysis (ED)
55 processes to treat wastewater, desalinate saline waters, and simultaneously produce electricity in a single
56 reactor (Cao et al., 2009; Qu et al., 2012; Cheng et al., 2017; Koók et al., 2017).

57 A typical MDC is fabricated from three chambers, anode, middle and cathode chambers, separated by
58 cation exchange membranes (CEM) and anion exchange membrane (AEM). In the anode chamber,
59 bacteria catalyze the oxidation of organic matter, release electrons from cell respiration, where they flow
60 towards the cathode through an external electrical circuit (Mehanna et al., 2010; An et al., 2014b). The
61 middle chamber contains an ion solution, and cathode chamber accepts the electrons received from anode
62 chamber (Cao et al., 2009; Saeed et al., 2015; Sevda et al., 2015). The potential difference between the

63 anode and cathode generates electricity, providing the driving force for water deionization (Jacobson et
64 al., 2011; Qu et al., 2012). Thus, loss of ionic species from the middle chamber results in desalination of
65 water without any external feed pressure, additional waste, and external electricity requirements.

66 In an MDC, the ion removal rate is affected by many factors, such as salt concentration, reactor volume,
67 retention time of wastewater and ion solution, membrane surface area, microbial oxidation rate, and the
68 ultimate electron acceptor used in cathode chamber (Luo et al., 2012b; Brastad and He, 2013; Meng et al.,
69 2014). So far, many catholytes or electron acceptors have been investigated in BESs. Cao et al. (2009)
70 used ferricyanide as the catholyte of MDC to desalinate water, and the maximum power density of 2 W
71 m^{-2} (31 W m^{-3}) was produced in their reactor. Although ferricyanide is an excellent catholyte in terms of
72 power density, it requires chemical regeneration and cannot be used for large-scale systems (Logan et al.,
73 2006). In other similar studies, the synthetic Cu(II) and Cr(VI)-containing wastewaters were chosen as the
74 cathodic electron acceptor, in which these compounds were rather competent in terms of current density
75 and desalination (An et al., 2014b, a). However, these cannot be used for desalination everywhere.

76 Mehanna et al. (2010) introduced air as an electron acceptor in a cathode chamber of a BES. Air-cathode
77 MDC reduced the conductivity of 5 g L^{-1} and 20 g L^{-1} NaCl solutions only by $43\pm 6\%$ and $50\pm 7\%$,
78 respectively. Zamanpour et al. (2017) used microalgae of *Chlorella vulgaris* as an oxygen generator in
79 MDC cathode chamber and observed the maximum power density of 20.25 mW m^{-2} in the system.
80 Nevertheless, there are still some ambiguities to be addressed; how to use certain oxidants with the ability
81 to accept electrons and which processes can be selected to improve the MDC performance.

82 According to what mentioned above, if the compounds with high redox potentials such as ozone are used
83 in the cathode chamber, it is expected to produce a more electrical current between cathode and anode,
84 which will increase the ion removal efficiency. So, this study aimed to evaluate the ozone capability as a
85 new cathodic electron acceptor in the MDC. The cell half-reactions and standard reduction potentials (E^0)
86 of ozone and oxygen in the bio-electrochemical systems are given in Eq. (1) and (2), respectively:



87 The obtained results in terms of salinity removal and electricity generation were compared with those of
88 another MDC operated with oxygen, O₂-MDC. Moreover, changes in morphology of anode surface
89 created by biofilm formation and microbial community existing in the reactors were investigated by
90 scanning electron microscopy (SEM) and 16S rRNA gene-sequencing techniques, respectively.

91 2. Material and methods

92 2.1 MDC configuration

93 All experiments on O₂-MDC and O₃-MDC were conducted independently in a 3-cell MDC, as shown in
94 Fig. 1. The reactor was constructed from polycarbonate blocks with a 5 cm diameter hole. The three
95 chambers were clamped together and separated by placing an AEM (AR204SXR412, Ionics, MA, USA)
96 between the anode and middle desalination chambers and a CEM (CR67, MK111, Ionics, MA, USA)
97 between the middle and cathode chambers. The anode electrode was a porous graphite (width × length =
98 25 mm × 30 mm) (Fuel Cell Store, Texas, USA) heated at 450 °C for 30 min and connected to a graphite
99 rod. Carbon cloth coated with 0.50 g cm⁻² Pt were used as the cathode electrode. After inserting the
100 electrodes, the volumes of anode, middle, and cathode chambers were 70, 38, and 70 mL, respectively.
101 The graphite electrode was washed using HCl (1 M) and subsequently with distilled water. The anode
102 was connected to the cathode by a piece of copper wire (10 cm). Also, membranes were pretreated to
103 expel their impurities and stabilize them. For this purpose, AEM and CEM were dipped in NaOH (1 M)
104 and HCl (1 M) solutions, respectively for 2 h. They were then rinsed thoroughly with distilled water.

105

106

Fig. 1

107

108 2.2 MDC start-up and operation

109 Before conducting desalination experiments, the reactor operated as a microbial fuel cell (MFC) for two
110 months with only one CEM between the anode and cathode chambers to form a satisfactory biofilm on
111 the anode surface. Then, the reactor was configured as microbial desalination cell. Anaerobic sludge
112 harvested from digestion tank of wastewater treatment plant (Yazd, Iran) was used to inoculate the anode
113 chamber. This chamber was also fed by a solution of Peptone water (25 g L⁻¹) and nutrients, including
114 (per liter in deionized water): 1.6 g C₆H₁₂O₆, 4.4 g KH₂PO₄, 3.4 g K₂HPO₄•3H₂O, 1.5 g NH₄Cl, 0.1 g
115 MgCl₂•6H₂O, 0.1 g CaCl₂•2H₂O, and 0.1 g KCl (all from Merck). The anode solution (anolyte) from an
116 external feed reservoir (100 mL) was continuously recirculated through the anode chamber at a rate of
117 0.05 mL min⁻¹ (HRT = 24 h) using two peristaltic pumps (M-RV Tygon, Etatron, Italy). In order to
118 maintain anaerobic condition, the anode chamber was purged with N₂ gas (40 mL min⁻¹) for 10 min and
119 sealed when the anode medium was injected into the chamber during the inoculation. The anolyte in the
120 feed bottle was replaced every 48 h to ensure the sufficient substrate is provided for the bacteria, and
121 avoid pH drop.

122 The middle chamber was filled with artificial salt water containing a NaCl solution (20 g L⁻¹),
123 representing a reasonable average salt concentration of seawater. The pre-treatment of NaCl solution was
124 carried out in an ultrasonic bath (model Transonic TI-H5, Elma, Germany) at the frequency of 22 kHz for
125 15 min.

126 The cathode chamber was filled with phosphate buffer as catholyte. To assess the ozone capability to
127 improve the efficacy of MDC, the catholyte was continuously diffused by ozone at the rate of 8.36 mg
128 min⁻¹. The achieved results in terms of salinity removal and electricity generation were compared with
129 those of O₂-MDC, which operated at the same condition. The ozone was generated in an ozone generator
130 (Ned Gas MK940, Netherlands) using oxygen (purity>95%) as input gas, and the ozone-laden flow was

131 diffused into the solution using diffuser installed at the bottom of the reactor. The operation of O₂-MDC
 132 and O₃-MDC with salt solution in the middle chamber continued until the voltage across the external
 133 resistance fell to 50 mV, and this was considered as one feeding cycle. The experiments were conducted
 134 at room temperature with normal atmospheric pressure and humidity. The O₂-MDC operated under open
 135 circuit voltage was used as control.

136 2.3 Analyses and calculation

137 Desalination efficiency was measured by monitoring the solution conductivity using a conductivity meter
 138 (HQ40d, HACH Co., USA), and results were then confirmed by a flame photometer (model CL378,
 139 Elico, India). The concentration of ozone in the inlet gas and off-gas streams was determined by sparging
 140 gas into a 2% KI solution and analyzing the solution by iodometric titration (APHA, 2005). Voltage (E,
 141 V) generated between anode and cathode as well as across the external resistance ($R_{ex}=200 \Omega$) was
 142 recorded every 5 min by a precision multimeter (Model 109N, APPA, Taiwan). The current (I, A) was
 143 also determined from the measured voltage according to Ohm's law ($I = E/R_{ex}$). Since the biological
 144 reactions take place in the anode chamber, the power density (P_{An} , W m⁻²) was calculated based on the
 145 cross-sectional area of anode electrode (A_{An} , m²) as follows (Logan et al., 2006; Logan, 2008):

$$146 \quad P_{An} = \frac{E^2}{A_{An}R_{ex}} \quad (3)$$

147 Furthermore, the polarization curves were measured by changing the external resistance from 10 Ω to 1
 148 M Ω (10 min per each resistor) with a resistance box (Rayannik, Ltd, Iran). The pH of solutions was
 149 determined by a Benchtop pH meter (HQd, HACH, USA). The total desalination rate (TDR, mg h⁻¹) was
 150 calculated by:

$$151 \quad TDR = \frac{(C_0 - C_t)V_d}{t} \quad (4)$$

152 where C_0 and C_t are the initial and final concentrations of NaCl, respectively; V_d (L) is the liquid volume
 153 within the desalination chamber, and t (h) is the time of desalination period.

154

155 2.3.1 SEM analysis

156 The morphology of biofilms formed on the anode electrode surface was analyzed by a scanning electron
157 microscopy (SEM, SUPRA 55VP - Carl Zeiss AG, Germany). Moisture had to be removed from the
158 biological samples by complete drying.

159

160 2.3.2 Bacterial Community Analysis

161 Bacterial community growth in the O₃-MDC was monitored by PCR-amplification of 16S rRNA genes
162 fragments. The samples were taken from anolyte and middle section of anode electrode. The thermal
163 shock method was used to extract DNA through following procedure: the anode samples were initially
164 placed at 100 °C for 10 min and then they were frozen for 10 min at -20 °C. This procedure was repeated
165 twice. Subsequently, samples were centrifuged (12000 rpm) for 10 min. The 16S rRNA genes of
166 extracted DNA were amplified by using the universal primer 338F (ACTCCTACGGGAGGCAGCA) and
167 806R (GGACTACHVGGGTWTCTAAT).

168 The substances final concentrations in 16S rRNA gene PCR reactions were 5 µl of sterile distilled water,
169 2 µl of each of the primers, 10 µl of Master Mix (Amplicon, Denmark), and 3 µl of extracted DNA. The
170 DNA qualities of the samples were evaluated with 1% agarose gel and TBE 0.5X electrophoresis beside
171 50bp Ladder.

172 The PCR thermal cycling scheme of 16S rRNA consisted of initial denaturation at 94 °C for 5 min,
173 followed by 35 cycles of denaturing at 94 °C for 45 s, annealing at 53 °C for 45 s, extending at 72 °C for
174 45 s, and a final extension for 5 min at 72 °C. PCR products of interest were then sent to the Macrogen
175 Company in South Korea for sequencing. The 16S rRNA sequences were analyzed and compared using

176 the Basic Local Alignment Search Tool (BLAST) in the NCBI GenBank database
177 (<http://www.ncbi.nlm.nih.gov/BLAST/>).

178 3. Results and discussion

179 3.1 Electricity generation and internal resistance

180 Fig. 2a and b shows the electrical profiles of MDCs operation. The open-circuit voltages (OCV) for 20 g
181 L⁻¹ NaCl desalination in O₂-MDC and O₃-MDC were 628 and 1331 mV, whereas the maximum closed
182 circuit voltages (200 Ω external resistor) were 178 and 793 mV, respectively. Each cycle of O₂-MDC and
183 O₃-MDC operation lasted about 66 and 94 h, respectively, indicating a more stable current profile in the
184 O₃-MDC. The maximum current density observed in the O₂-MDC was 1.16 A m⁻²; however, it increased
185 to 5.27 A m⁻² when ozone was used in the MDC. The current densities of O₃-MDC were higher than O₂-
186 MDC in all operation times. Also, this parameter increased in both reactors during the lag phase of
187 operation, then, declined after rising to peak value. However, the initial declining slope was greater in O₃-
188 MDC. Such electrical trend is almost observed in MDC studies because the internal resistance gradually
189 increases because of conductivity drop during desalination and substrate consumption (Luo et al., 2012a;
190 Yuan et al., 2016; Sevda et al., 2017). Furthermore, the consequent higher salt concentration in the
191 anolyte could inhibit microbial activity (Sevda et al., 2017).

192 Fig. 2

193
194 In MFCs and MDCs, many important information and conditions of reactors, such as internal resistance,
195 can be derived from polarization curve, which represents the voltage versus the current (density). Internal
196 resistance is an important factor controlling the power generation of BESs. In a microbial desalination
197 cell, the slope of the polarization curve gives the internal resistance of reactor. Also, the maximum power
198 density is achieved when the internal and external resistances are equal (Logan et al., 2006; Logan, 2008).

199 As shown in Fig. 3, the power density improved by the increase of current density and reached to the
200 highest level. After this point, because of increasing in electrons resistance passing through the electrodes
201 as well as in interconnections and over-sizing the potential of electrodes, the power density decreased. A
202 maximum power density of 4.06 W m^{-2} was observed in the O_3 -MDC, which was about 11 times higher
203 than that obtained in O_2 -MDC (0.369 W m^{-2}). The higher redox potential of ozone (2.07 V) than oxygen
204 (1.23 V) can significantly justify such findings. In practical phase, ozone diffusion into catholyte would
205 be ecologically sound, leaves no dangerous trace, and maintains its efficacy in a wide range of pH. In a
206 BES, ozone breaks down into oxygen within a short time; this oxygen will again participate in the
207 reaction. In addition, in the next applications of O_3 -MDC, industrial wastewater containing ionic pollutant
208 can enter into the middle chamber instead of saline water, the ions transferred from middle chamber
209 would be rapidly oxidized by the ozone, which reduced its toxicity further.

210 The internal resistances of 305 and 71Ω were estimated, respectively for O_2 -MDC and O_3 -MDC. In
211 practice, the internal resistance of a BES influences strongly the electric current output and depends on
212 many factors, such as the material used for anode and cathode electrode, reactor size, chemical
213 properties, temperature, electrolyte conductivity, ion mobility, and electrode surface area (Heijne et al.,
214 2010; Saeed et al., 2015; Sevda et al., 2017). Liang et al. (2008) used carbon nanotube, flexible graphite
215 and activated carbon as anode material of MFC, and found that the internal resistances were 263, 301 and
216 381Ω , respectively. Min and Angelidaki (2008) constructed an MFC in which an anode electrode and a
217 cathode chamber were immersed in the anaerobic reactor; they found that the internal resistance was 35
218 Ω . Kim et al. (2007) found that the membrane type can influence the maximum power densities, and
219 internal resistances of air-cathode cube MFCs ($84\text{-}91 \Omega$) were lower than aqueous-cathode bottle MFCs
220 ($1230\text{-}1272 \Omega$). However, in this study, the use of O_3 -MDC for desalination resulted in a reduction in
221 internal resistance as compared with O_2 -MDC. Employing narrower middle chambers would reduce the
222 internal resistance and improve the power generation and ion removal (Kim and Logan, 2013). These

223 results demonstrate higher efficiency of ozone in terms of power production compared to oxygen as
224 electron acceptors in the reactor.

225

226 **Fig. 3**

227

228 3.2 The desalination performance of MDCs

229 In terms of salt removal in O₃-MDC, it was determined that the desalination efficiency is a function of
230 current generation in different stages; accordingly, a faster desalination was achieved under higher current
231 generation (Fig. 4). The O₂-MDC and O₃-MDC had the average TDR of 2.02±0.21 and 2.58±0.34 mg
232 TDS h⁻¹, respectively. In the initial 24 h of operation, the O₂-MDC and O₃-MDC removed more than
233 18.99% and 35.80% of the salt from the middle chamber and their TDRs were 3.69±0.4 and 5.00±0.45
234 mg TDS h⁻¹, respectively. However, TDR reduced by the increase of the operation time due to the
235 reduction of active ions in the middle chamber. Moreover, the gradual increase in the anolyte conductivity
236 is detrimental to the microorganisms and can hinder microbial activity. As a result, the desalination rate is
237 reduced (Luo et al., 2012a). O₂-MDC produced an average current of 0.42±0.02 mA and removed
238 55.58±0.2% of salt from middle chamber solution during operation time. The performance of O₂-MDC
239 was similar to other previous MDC systems operated using air (Mehanna et al., 2010) or ferricyanide
240 (Luo et al., 2012b). However, when ozone was used in the MDC, the average current of 1.41±0.3 mA and
241 74.08±3.1% of desalination were obtained. This indicates about 18% enhancement in desalination
242 performance.

243 The conductivity of anolyte increased from 8.4 to 14.6 mS cm⁻¹ during one desalination cycle. This
244 increase was most probably due to the movement of anions available in middle solution toward anode
245 chamber during desalination. In the open circuit control, O₂-MDC and O₃-MDC eliminated only up to

246 19% and 21% of salt, respectively, indicating desalination was mainly due to the generation of electric
247 current, and other factors such as natural osmosis, ion exchange, and scale formation had minor
248 involvement.

249 However, the obtained desalination efficiencies in O₃-MDC are higher than many of the values observed
250 in previous studies. For example, in a study in which ferricyanide was used as the electron acceptor, the
251 MDC removed about 66% of the salt from the middle chamber during 400 h of operation, and in long-
252 term operation, the current density and desalination rate decreased by 47% and 27%, respectively (Luo et
253 al., 2012a). In another study, Sevda et al. (2017) obtained the maximum desalination efficiency of 19.9%
254 in an MDC operated with real seawater and phosphate buffer solution as catholyte. This indicates that
255 using MDCs with ozone as an electron acceptor in the catholyte chamber can provide sufficient energy
256 for downstream desalination processes, e.g., reverse osmosis.

257

258 **Fig. 4**

259

260 3.3 Biofilm Formation on Anode Surface

261 Micrographs of anode surface before and after the experiment were recorded by a software-controlled
262 digital SEM to observe the biofilm formation. A close inspection of Fig. 5a and b displays a significant
263 change in morphology of anode electrode, so that the fresh anode electrode had a clear surface, while the
264 SEM images of the used anode indicated occupation of microbes on the electrode surface. The anode
265 biofilm had a complex dense structure distributed on the whole surface of graphite.

266

266 **Fig. 5**

267

268 3.4 Microbial Community Analysis

269 16S rRNA gene-based high-throughput sequencing, which is known as an effective method to analyze
270 microbial community structures and functions in MFCs and MDCs was used to illustrate the dependence
271 of bacterial communities and their relationships (Zhi et al., 2014; Liu et al., 2015). Both anode electrode
272 and anolyte solution of O₃-MDC were sampled and sequenced in this study. Table 1 summarizes the
273 identified names of bacterial families present in the anode biofilm and anolyte. The anode biofilm had
274 more diverse microbial community than anolyte sample. Proteobacteria were dominated microbial
275 communities both in the anode biofilm and anolyte sample. Firmicutes and Acidobacteria were other
276 microbial communities detected in BLAST results of anode biofilm sample, while were not identified in
277 the anolyte. The Proteobacteria of anode biofilm belonged to betaproteobacteria and
278 gammaproteobacteria classes. However, epsilonproteobacteria and Bacteroidia were only classes existed
279 in anolyte sample. Proteobacteria species were widely reported in previous MFC and MDC studies and
280 were considered as the dominant exoelectrogenic bacteria presumably due to competitive advantages in
281 extracellular electron transfer (Luo et al., 2012a; Luo et al., 2012b; Liu et al., 2015; Zhang et al., 2016).
282 Bacteroidetes are gram-negative, anaerobic or aerobic, and rod-shaped bacteria that were widely reported
283 in the anode of BESs and seawater (Lu et al., 2012; Gao et al., 2014). The presence of Acidobacteria may
284 be a result of low pH of the O₃-MDC anolyte, because these species were reported capable of
285 withstanding acidic, metal-contaminated, and other extreme environments (Barns et al., 2007). Firmicutes
286 are obligate anaerobic bacteria, which can consume glucose and convert it to acetate, lactate, butyrate,
287 ethanol, CO₂ and H₂ (Ludwig et al., 2009; Karluvali et al., 2015). Rabaey and Verstraete (2005) suggested
288 some species of gammaproteobacteria and Firmicutes poses capacity to generate electricity. The anode
289 biofilm also contained uncultured marine bacterium, which may be attributed to the higher salinity in the
290 MDC anode chamber.

291 Due to some limitations, this study only focused on the microbial community excised in anode and
292 anolyte samples at the family level. It is recommended that in the subsequent studies, the sample is first

293 cultured in the special culture medium, and after taking the single typical colonies, more comprehensive
294 characterizations be conducted using high throughput sequencing technologies such as pyrosequencing to
295 observe the distribution and contribution of each species in the microbial community.

296

297

Table 1

298 4. Conclusion

299 Salinity removal and electricity generation were successfully accomplished in the MDC with ozone as a
300 new cathode electron acceptor. The salinity removal and electricity generation data of O₃-MDC were
301 compared with those achieved through O₂-MDCs. Results showed faster desalination was occurred under
302 higher current generation. The O₂-MDC performance was similar to other MDCs operated previously.
303 However, when ozone was used as an electron acceptor, the reactor had lower internal resistance, the
304 desalination performance enhanced, and the current density and power density were several times higher
305 than those obtained in O₂-MDC. The results recommend ozone cathode MDC as a promising technology,
306 both for seawater desalination and bio-electricity generation during wastewater treatment, especially as a
307 pre-treatment mechanism for membrane processes.

308

309 Acknowledgement

310 This study was financially supported by grant No: 951205 of the Biotechnology Development Council of
311 the Islamic Republic of Iran, and Shahid Sadoughi University of Medical Sciences (Grant No: 12532).

312 References

313 An, Z., Zhang, H., Wen, Q., Chen, Z., Du, M., 2014a. Desalination combined with copper(II) removal in
314 a novel microbial desalination cell. *Desalination* 346, 115-121.

- 315 An, Z., Zhang, H., Wen, Q., Chen, Z., Du, M., 2014b. Desalination combined with hexavalent chromium
316 reduction in a microbial desalination cell. *Desalination* 354, 181-188.
- 317 APHA, 2005. Standard methods for the examination of water and wastewater. AWWA, Washington, DC.
- 318 Barns, S.M., Cain, E.C., Sommerville, L., Kuske, C.R., 2007. Acidobacteria phylum sequences in
319 uranium-contaminated subsurface sediments greatly expand the known diversity within the phylum. *Appl.*
320 *Environ. Microbiol.* 73, 3113-3116.
- 321 Brastad, K.S., He, Z., 2013. Water softening using microbial desalination cell technology. *Desalination*
322 309, 32-37.
- 323 Burn, S., Hoang, M., Zarzo, D., Olewniak, F., Campos, E., Bolto, B., Barron, O., 2015. Desalination
324 techniques - A review of the opportunities for desalination in agriculture. *Desalination* 364, 2-16.
- 325 Cao, X., Huang, X., Liang, P., Xiao, K., Zhou, Y., Zhang, X., Logan, B.E., 2009. A new method for water
326 desalination using microbial desalination cells. *Environ. Sci. Technol.* 43, 7148-7152.
- 327 Cheng, Y., Wang, L., Faustorilla, V., Megharaj, M., Naidu, R., Chen, Z., 2017. Integrated electrochemical
328 treatment systems for facilitating the bioremediation of oil spill contaminated soil. *Chemosphere* 175,
329 294-299.
- 330 Gao, C., Wang, A., Wu, W.-M., Yin, Y., Zhao, Y.-G., 2014. Enrichment of anodic biofilm inoculated
331 with anaerobic or aerobic sludge in single chambered air-cathode microbial fuel cells. *Bioresour. Technol.*
332 167, 124-132.
- 333 Gholizadeh, A., Mokhtari, M., Naimi, N., Shiravand, B., Ehrampoush, M.H., Miri, M., Ebrahimi, A.,
334 2017. Assessment of corrosion and scaling potential in groundwater resources; a case study of Yazd-
335 Ardakan Plain, Iran. *Groundwat. Sustain. Dev.* 5, 59-65.
- 336 Heijne, A.T., Liu, F., Weijden, R.v.d., Weijma, J., Buisman, C.J., Hamelers, H.V., 2010. Copper recovery
337 combined with electricity production in a microbial fuel cell. *Environ. Sci. Technol* 44, 4376-4381.
- 338 Jacobson, K.S., Drew, D.M., He, Z., 2011. Efficient salt removal in a continuously operated upflow
339 microbial desalination cell with an air cathode. *Bioresour. Technol.* 102, 376-380.
- 340 Karluvalı, A., Koroğlu, E.O., Manav, N., Çetinkaya, A.Y., Özkaya, B., 2015. Electricity generation from
341 organic fraction of municipal solid wastes in tubular microbial fuel cell. *Sep. Purif. Technol.* 156, 502-
342 511.
- 343 Kim, J.R., Cheng, S., Oh, S.E., Logan, B.E., 2007. Power generation using different cation, anion, and
344 ultrafiltration membranes in microbial fuel cells. *Environ. Sci. Technol.* 41, 1004-1009.
- 345 Kim, Y., Logan, B.E., 2013. Microbial desalination cells for energy production and desalination.
346 *Desalination* 308, 122-130.
- 347 Koók, L., Nemestóthy, N., Bakonyi, P., Zhen, G., Kumar, G., Lu, X., Su, L., Saratale, G.D., Kim, S.-H.,
348 Gubicza, L., 2017. Performance evaluation of microbial electrochemical systems operated with Nafion
349 and supported ionic liquid membranes. *Chemosphere* 175, 350-355.

- 350 Liang, P., Fan, M.Z., Cao, X.X., Huang, X., Peng, Y.M., Wang, S., Gong, Q.M., Liang, J., 2008.
351 Electricity generation by the microbial fuel cells using carbon nanotube as the anode. *Huan jing ke xue*
352 29, 2356-2360.
- 353 Liu, G., Zhou, Y., Luo, H., Cheng, X., Zhang, R., Teng, W., 2015. A comparative evaluation of different
354 types of microbial electrolysis desalination cells for malic acid production. *Bioresour. Technol.* 198, 87-
355 93.
- 356 Logan, B.E., 2008. *Microbial Fuel Cells*. John Wiley & Sons, Inc., Hoboken, New Jersey.
- 357 Logan, B.E., Hamelers, B., Rozendal, R., Schröder, U., Keller, J., Freguia, S., Aelterman, P., Verstraete,
358 W., Rabaey, K., 2006. Microbial fuel cells: methodology and technology. *Environ. Sci. Technol.* 40,
359 5181-5192.
- 360 Lu, L., Xing, D., Ren, N., 2012. Pyrosequencing reveals highly diverse microbial communities in
361 microbial electrolysis cells involved in enhanced H₂ production from waste activated sludge. *Water res.*
362 46, 2425-2434.
- 363 Ludwig, W., Schleifer, K.-H., Whitman, W.B., 2009. Revised road map to the phylum Firmicutes.
364 *Bergey's Manual® of Systematic Bacteriology*. Springer, pp. 1-13.
- 365 Luo, H., Xu, P., Ren, Z., 2012a. Long-term performance and characterization of microbial desalination
366 cells in treating domestic wastewater. *Bioresour. Technol.* 120, 187-193.
- 367 Luo, H., Xu, P., Roane, T.M., Jenkins, P.E., Ren, Z., 2012b. Microbial desalination cells for improved
368 performance in wastewater treatment, electricity production, and desalination. *Bioresour. Technol.* 105,
369 60-66.
- 370 Mehanna, M., Saito, T., Yan, J., Hickner, M., Cao, X., Huang, X., Logan, B.E., 2010. Using microbial
371 desalination cells to reduce water salinity prior to reverse osmosis. *Energy. Environ. Sci.* 3, 1114-1120.
- 372 Meng, F., Jiang, J., Zhao, Q., Wang, K., Zhang, G., Fan, Q., Wei, L., Ding, J., Zheng, Z., 2014.
373 Bioelectrochemical desalination and electricity generation in microbial desalination cell with dewatered
374 sludge as fuel. *Bioresour. Technol.* 157, 120-126.
- 375 Min, B., Angelidaki, I., 2008. Innovative microbial fuel cell for electricity production from anaerobic
376 reactors. *J. Power Sources* 180, 641-647.
- 377 Ping, Q., Zhang, C., Chen, X., Zhang, B., Huang, Z., He, Z., 2014. Mathematical model of dynamic
378 behavior of microbial desalination cells for simultaneous wastewater treatment and water desalination.
379 *Environ. Sci. Technol.* 48, 13010-13019.
- 380 Qu, Y., Feng, Y., Wang, X., Liu, J., Lv, J., He, W., Logan, B.E., 2012. Simultaneous water desalination
381 and electricity generation in a microbial desalination cell with electrolyte recirculation for pH control.
382 *Bioresour. Technol.* 106, 89-94.
- 383 Rabaey, K., Verstraete, W., 2005. Microbial fuel cells: novel biotechnology for energy generation. *Trends*
384 *Biotechnol.* 23, 291-298.

- 385 Saeed, H.M., Hussein, G.A., Yousef, S., Saif, J., Al-Asheh, S., Abu Fara, A., Azzam, S., Khawaga, R.,
386 Aidan, A., 2015. Microbial desalination cell technology: A review and a case study. *Desalination* 359, 1-
387 13.
- 388 Sevda, S., Abu-Reesh, I.M., Yuan, H., He, Z., 2017. Bioelectricity generation from treatment of
389 petroleum refinery wastewater with simultaneous seawater desalination in microbial desalination cells.
390 *Energy Convers. Manage.* 141, 101-107.
- 391 Sevda, S., Yuan, H., He, Z., Abu-Reesh, I.M., 2015. Microbial desalination cells as a versatile
392 technology: functions, optimization and prospective. *Desalination* 371, 9-17.
- 393 Yuan, H., Abu-Reesh, I.M., He, Z., 2016. Mathematical modeling assisted investigation of forward
394 osmosis as pretreatment for microbial desalination cells to achieve continuous water desalination and
395 wastewater treatment. *J. Memb. Sci.* 502, 116-123.
- 396 Zamanpour, M.K., Kariminia, H.-R., Vosoughi, M., 2017. Electricity generation, desalination and
397 microalgae cultivation in a biocathode-microbial desalination cell. *J. Environ. Chem. Eng.* 5, 843-848.
- 398 Zhang, H., Wen, Q., An, Z., Chen, Z., Nan, J., 2016. Analysis of long-term performance and microbial
399 community structure in bio-cathode microbial desalination cells. *Environ. Sci. Pollut. Res.* 23, 5931-5940.
- 400 Zhi, W., Ge, Z., He, Z., Zhang, H., 2014. Methods for understanding microbial community structures and
401 functions in microbial fuel cells: a review. *Bioresour. Technol.* 171, 461-468.
- 402
- 403

Figure captions:

Fig. 1: Three-chamber MDC used for desalination tests: (a) schematic, and (b) actual image.

Fig. 2: Electrical profiles during operation: (a) O₂-MDC, and (b) O₃-MDC (salt water concentration of 20 g L⁻¹, and external resistor of 200 Ω).

Fig. 3: Polarization and power density curves of (a) O₂-MDC, and (b) O₃-MDC

Fig. 4: Desalination efficiency and TDR of O₂-MDC and O₃-MDC

Fig. 5: SEM image: (a) anode surface before the experiments (5000x), and (b) anode surface after the experiments (7500x)

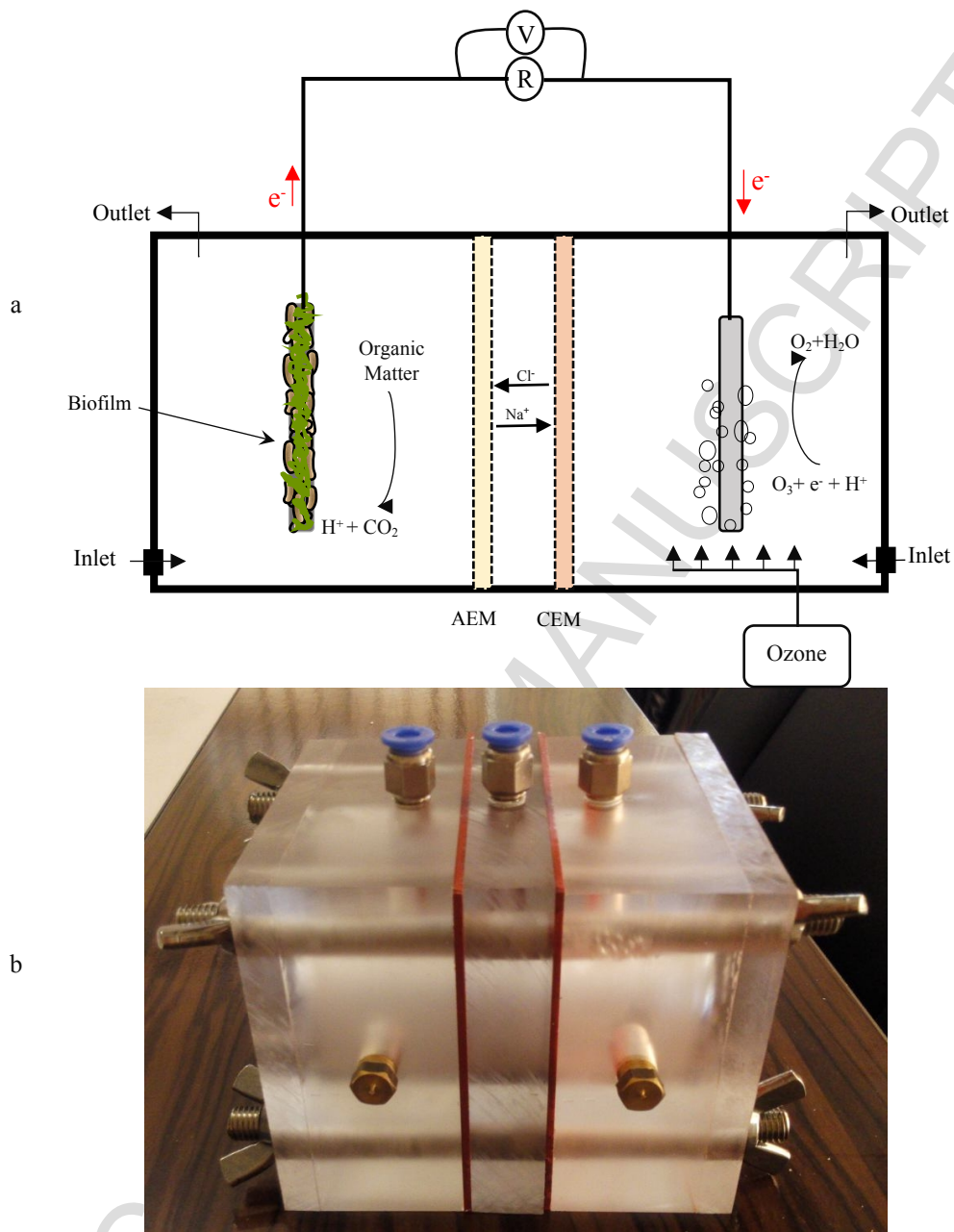
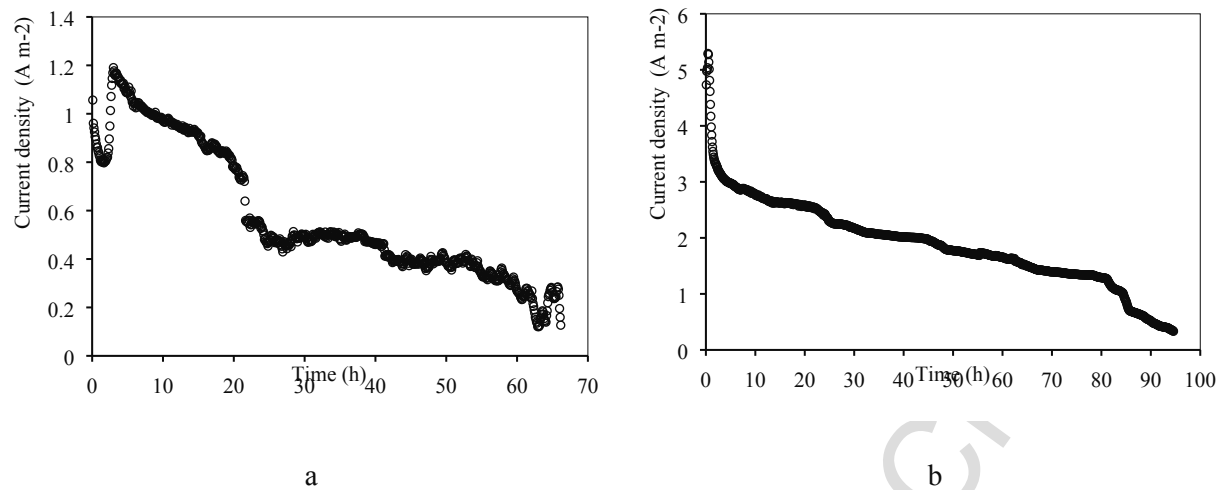


Fig. 1:

**Fig. 2:**

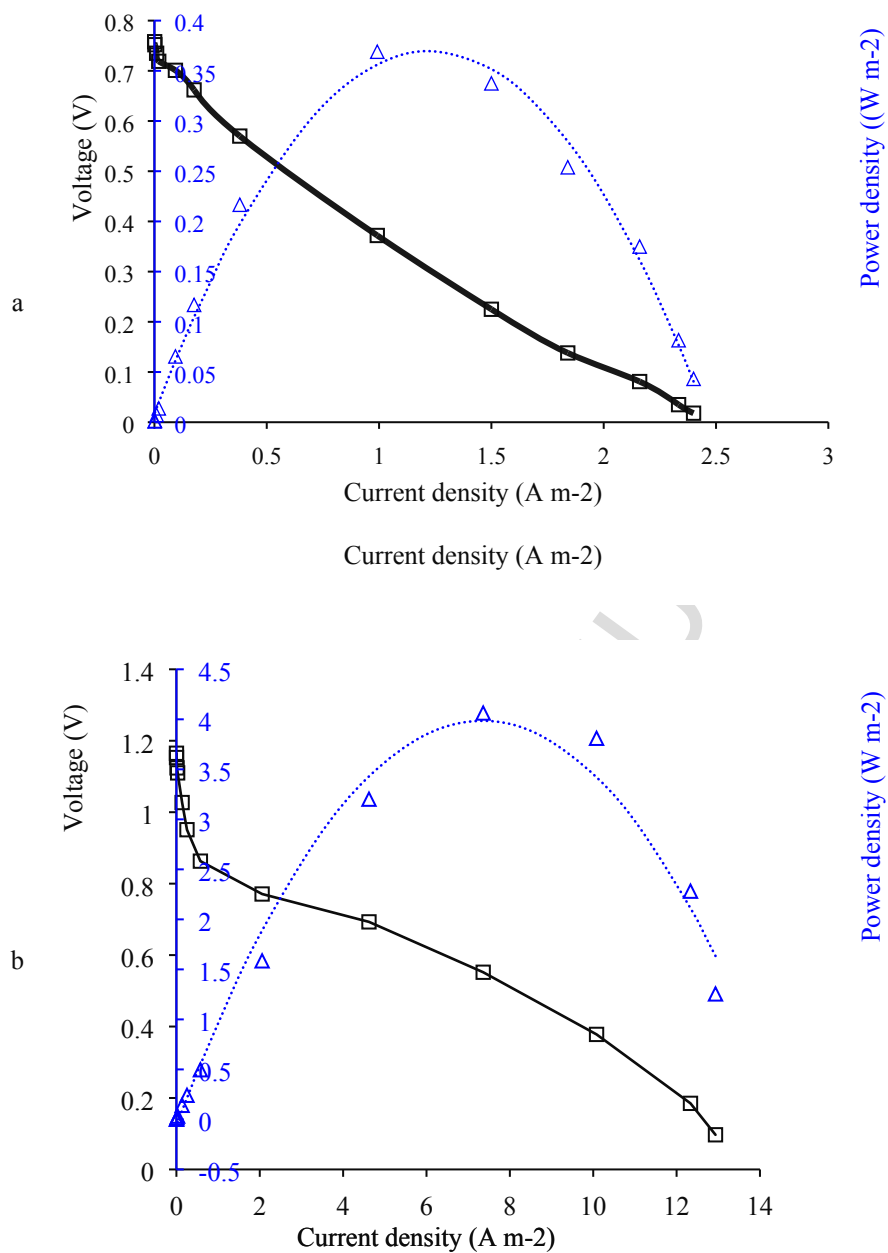


Fig. 3:

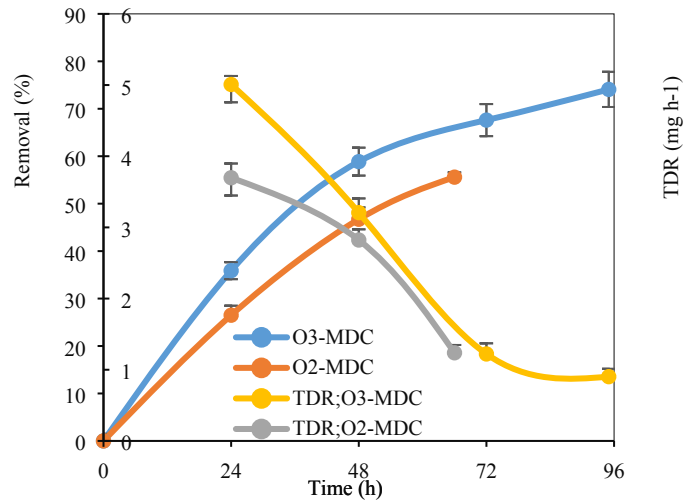


Fig. 4:

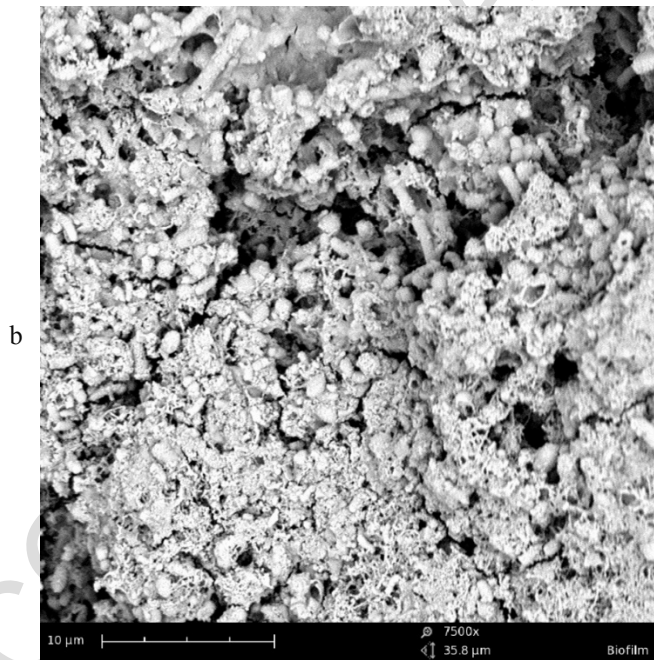
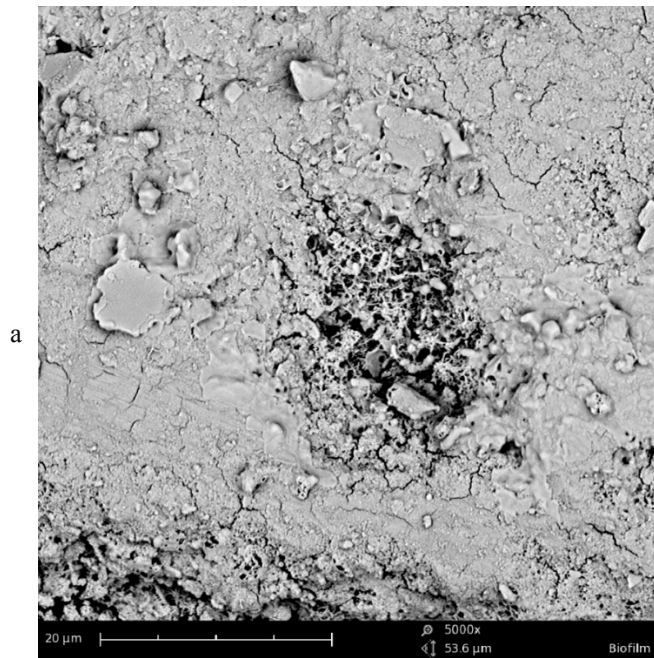


Fig. 5:

Table caption:

Table 1: Bacterial community of O₃-MDC's anode and anolyte samples.

ACCEPTED MANUSCRIPT

Table 1:

Sequence ID	Family	Class	Phylum	Similarity (%)	GenBank accession No.
Anode biofilm					
MA1	Acidobacteriaceae	Acidobacteria	Acidobacteria	88	HG763957.1
MA2	Chromatiaceae	Gammaproteobacteria	Proteobacteria	91	HQ877094.1
MA3	Ectothiorhodospiraceae	Gammaproteobacteria	Proteobacteria	87	KC009941.1
MA4	Burkholderiaceae	Betaproteobacteria	Proteobacteria	87	KP772724.1
MA5	Clostridiaceae	Clostridia	Firmicutes	89	KU045501.1
Anolyte					
MS1	Campylobacteraceae	Epsilonproteobacteria	Proteobacteria	89	KF721645.1
MS2	Prevotellaceae	Bacteroidia	Bacteroidetes	86	GU955392.1